ANNALS of the ORADEA UNIVERSITY.

Fascicle of Management and Technological Engineering, Volume VII (XVII), 2008

STUDY ON EFFICIENCY OF AN PARABOLIC REFLECTIVE SOLAR CONCENTRATOR

Corina GRUESCU[1], Renata BODEA[2], Marius COSTACHE[1]
[1]University Politehnica Timisoara, Mechatronics Department
[2]University of Oradea, Mechatronics and Fine Mechanics Department
e-mail: corina_gruescu@yahoo.com, prod.conf@rdslink.ro

Keywords: solar static 3D concentrator, modelling and simulating, optical concentration coefficient

Abstract: The paper presents a numerical simulation to determine the optimal geometry of a 3D paraboloid solar concentrator. The results show that aperture and height are interdependent and are determined by the paraboloid constant p. The optimal position of the cell also depends on the value of p. Cell's best abscissa is not the paraxial one, a defocusing being absolutely necessary. The paper provides a fully determined solution for a 3D paraboloid concentrator, chose from a family of surfaces, for which the aperture, the height, the cell diameter and the parabola constant are parameters.

1. INTRODUCTION

Solar energy, converted into electrical or/and thermal energy might replace traditional electrical sources. In some cases it is an alternative source, while in other cases it represents the only solution. Due to wide capture surfaces, light concentrators are absolutely necessary to reduce the size of the solar installation.

Solar light concentrators represent an assembly of a solar or photovoltaic cell, which aims to convert solar energy into electrical one.

The concentrator is a non – imaging optical system, designed to gather and concentrate as efficient as possible the solar energy.

The central concept in the theory of photovoltaic cells is a spectral radiometric size – the spectral irradiance. At the surface of the sun, the integral irradiance is ~6.3 $kWcm^{-2}$. It decreases proportionally with the square distance so that at the atmosphere entrance it is ~137$mWcm^{-2}$. Depending on atmospherically conditions, at the level of the ground the irradiance is 80...100 $mWcm^{-2}$. This value is multiplied by the concentrators. Only non – imaging devices assure high concentrating coefficients.

Word – wide, solar power is used for obtaining electricity. Table 1 shows the total power of installed solar cells at the end of 2005, which was a peak year [1].

Table 1 Total power of installed solar cells at the end of 2005 in the main countries using solar cell technology

Country	Total power [kW]	Of which in 2005 [kW]
Germany	1.429.000	635.000
Japan	1.421.908	289.917
USA	479.000	103.000
Australia	60.581	8.280
Spain	57.400	20.400
Netherlands	50.776	1.697
Italy	37.500	6.800

2. GEOMETRICAL PARAMETERS OF A PARABOLIC CONCENTRATOR

There are different types of concentrators (2D or 3D, static or dynamic, reflecting or refractive).

The parabolic concentrator is a 3D, static, reflecting kind of concentrator. It is not

very simple to manufacture and thus not very cheap, but if proper designed, it may be very efficient. The receiving element of energy is situated nearby the focal area.

The optical concentration coefficient depends on the aperture of the paraboloid, on the defocusing of the receiver and in the incidence angle of the light beam [2], [3].

The concentrator is a rotation surface, whose generator is a parabola (figure 1).

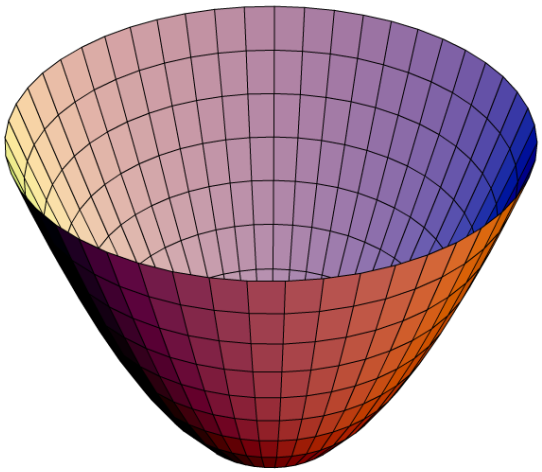

Fig. 1. Paraboloid surface

The parabola is a plane curve, belonging to the family of quadric surfaces, whose equation in a (R, H) system is [4]:

$$H = \frac{1}{r} \cdot \frac{R^2}{1 + \sqrt{1 - (k+1)\frac{R^2}{r^2}}}, \tag{1}$$

where k is the quadric constant and r – the radius of the circle tangent to the vertex.

For the parabola: k= - 1

$$\Rightarrow H = \frac{R^2}{2r} \text{ or } R^2 = 2rH \text{ or } R^2 = 2pH. \tag{2}$$

In equation (2) the radius r was replaced with the symbol p in order to emphasise its parametric character. During the further studies it is going to be a variable.

Figure 2 represents an arch of parabola, the circle tangent to the vertex. The dimensions of the entrance and exit apertures (a and a') are drawn. The exit aperture indicates the plane where the receiver is placed.

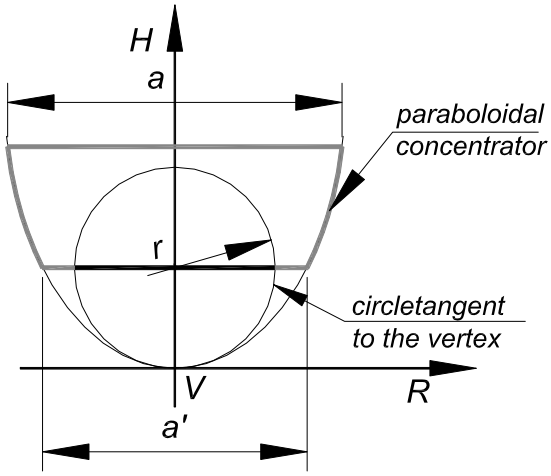

Fig. 2. Geometric elements of a parabolic concentrator

In the paraxial area, the aspheric components have the characteristics of the spherical surface, tangent to the vertex. For the spherical mirror the focal length is:

$$f = \frac{r}{2} = \frac{p}{2}. \tag{3}$$

Hence, the paraxial abscissa of the receiver is equal to f. The radius of the receiver results from the equation of the parabola, where H=f:

$$R_{det}^2 = 2p \cdot \frac{p}{2} = p^2 \Rightarrow R_{det} = p. \tag{4}$$

Thus, the parameter p is chosen equal to the radius of the light detector. On average radius for the receiver is R_{det} = *20* mm, so that:

$$p = R_{det} = 20\ mm. \tag{5}$$

The exit aperture results:

$$a' = 2R_{det} = 40\,mm \tag{6}$$

and the equation of the generating parabola becomes:

$$R^2 = 40H. \tag{7}$$

The preliminary position of the detector is set for the paraxial abscissa *H* = *f* = 10 mm. The study is going to search the optimal place of the cell by means of defocusing.

A complete geometry of the concentrator needs the establishment of another two sizes: aperture *a* and height H. The relation between these sizes is:

$$H = \frac{a^2}{8p} - \frac{p}{2}. \tag{8}$$

In relation (8) one of the variables needs to be assumed. The study starts with three apertures: Φ60, Φ80 and Φ120 mm. These values lead to a family of concentrators, whose characteristics are presented in table 2. Plots of corresponding surfaces are given in figures 3, 4 and 5.

Table 2. Geometric characteristic of concentrators family

p	20	20	20
f	10	10	10
a'/2	20	20	20
H_f	10	10	10
a/2	30	40	60
H	12.5	30	80

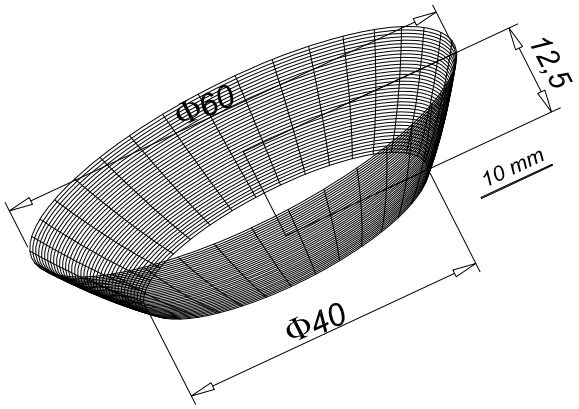

Fig. 3. Parabolic concentrator (p=20, a=60, a'=40, H=12.5)

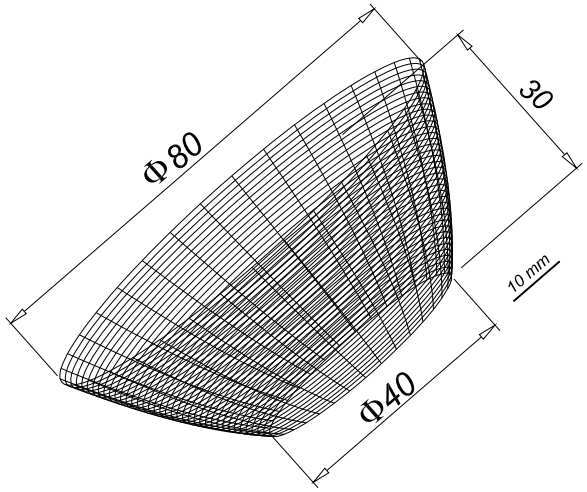

Fig. 4. Parabolic concentrator (p=20, a=80, a'=40, H=30)

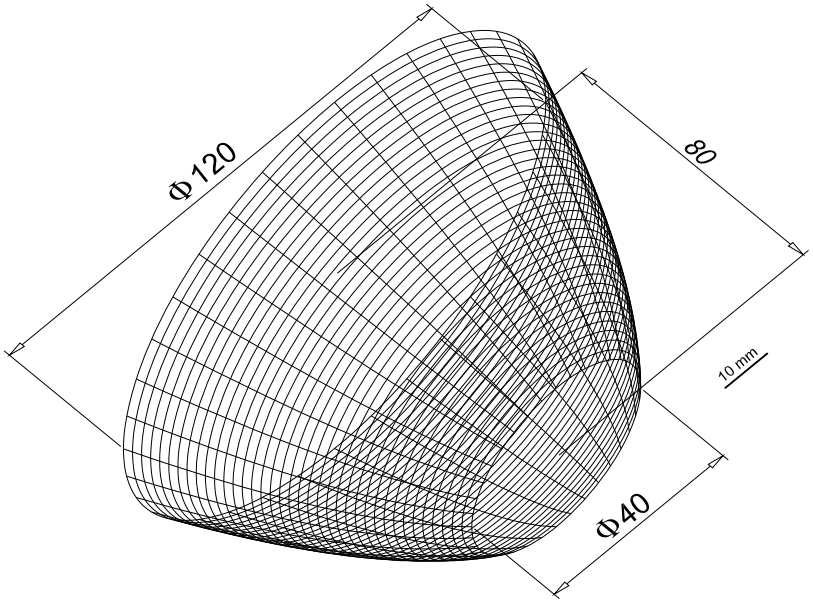

Fig. 5. Parabolic concentrator (p=20, a=120, a'=40, H=80)

3. MODELLING AND SIMULATION

Considering a normalized intensity of the incident rays, I_0=100 and a reflection coefficient ρ=0.94, the scanning of a *90*^{o} field was simulated. The light beam was shared accordingly to a mesh sized *10*x*10* for all apertures. The simulation needed special software, written on the basis of the generalized Ray Tracing method [5].

The receiving element is round and presents an active zone with the diameter Φ40mm

The final goal of the study is the variation of the optical concentration coefficient in respect with the paraboloid's aperture and position of the receiving cell.

Tables 3…5 present the results of simulations for *a*=60, 80 respectively 120 mm and for detector's abscissa H_{det}=10, 15, 20 and 25 mm.

Column *0* indicates the abscissa of the receiving cell. Next column contains the incidence angles within the range 0...90^o, step 10^o. Column 2 gives the values of the normated energetic size, measured at the surface of the cell. The last two columns indicate the number of the absorbed radii by the cell, respectively the number of radii

multiply reflected on the surface of the mirror, which gets out of the system without reaching the cell.

Table 3. Results of simulation for aperture=60 mm

	θ [°]	I [-]	Nr. of absorbed rays [-]	Nr. of rays emerging from the system after multiple reflexions [-]
0	1	2	3	4
H_{det} = 10, p=20, a=60, H=12.5, C_S=1.5	0	126.78	18203	0
	10	118.44	14433	3770
	20	105.86	12387	5816
	30	87.45	11013	7190
	40	63.2	9506	8697
	50	38.02	7761	10442
	60	17.28	5610	12593
	70	3.55	2453	15750
	80	0	0	18203
	90	0	0	18203
H_{det} = 15, p=20, a=60, H=12.5, C_S=1.5	0	177.64	18203	0
	10	150.88	16776	1427
	20	119.19	14020	4183
	30	89.03	11541	6662
	40	64.78	9950	8253
	50	42.6	8682	9521
	60	24.1	7926	10277
	70	8.47	5860	12343
	80	0.31	843	17360
	90	0	0	18203
H_{det} = 20, p=20, a=60, H=12.5, C_S=1.5	0	215.22	18203	0
	10	183.52	16245	1958
	20	122.69	13318	4885
	30	84.93	11093	7110
	40	64.08	10087	8116
	50	45.52	9443	8760
	60	30.1	9279	8924
	70	14.69	9036	9167
	80	2.77	7425	10778
	90	0	0	18203
H_{det} = 25, p=20, a=60, H=12.5, C_S=1.5	0	215.22	18203	0
	10	191.55	16941	1262
	20	108.02	10230	7973
	30	78.38	9878	8325
	40	65.42	10666	7537
	50	50.89	10591	7612
	60	36.71	10512	7691
	70	23.89	11679	6524
	80	4.01	8073	10130
	90	0	0	18203

Table 4. Results of simulation for aperture a=80 mm

	θ [°]	I [-]	Nr. of absorbed rays [-]	Nr. of rays emerging from the system after multiple reflexions [-]
0	1	2	3	4
H_{det} = 10, p=20, a=80, H=40, C_S=2	0	211.82	18090	0
	10	193.9	15447	2643
	20	141.04	9983	8107
	30	94.99	7074	11015
	40	55.98	4755	13335
	50	23.88	2614	15476
	60	3	542	17548
	70	0	0	18090
	80	0	0	18090
	90	0	0	18089
H_{det} = 15, p=20, a=80, H=40, C_S=2	0	262.62	18090	0
	10	229.66	17293	797
	20	149.71	11227	6863
	30	93.34	7164	10925
	40	63.99	5499	12591
	50	32.87	3792	14298
	60	8.7	1575	16515
	70	0	0	18090
	80	0	0	18090
	90	0	0	18089
H_{det} = 20, p=20, a=80, H=40, C_S=2	0	319.63	18090	0
	10	264.32	16406	1684
	20	154.98	12344	5746
	30	90.07	7211	10878
	40	63.86	5662	12428
	50	41.56	4859	13231
	60	15.81	2898	15192
	70	0.71	275	17815
	80	0	0	18090
	90	0	0	18089
H_{det} = 25, p=20, a=80, H=40, C_S=2	0	376.49	18090	0
	10	289.69	15850	2240
	20	145.62	10310	7780
	30	83.27	6987	11102
	40	65.31	6093	11997
	50	48.26	5696	12394
	60	22.51	4102	13988
	70	4.78	1847	16243
	80	0	0	18090
	90	0	0	18089

Table 5. Results of simulation for aperture a=120 mm

	θ [°]	I [-]	Nr. of absorbed rays [-]	Nr. of rays emerging from the system after multiple reflexions [-]
0	1	2	3	4
H_{det} = 10, p=20, a=120, H=80, C_S=3	0	559.27	18203	0
	10	452.76	14869	3334
	20	170.97	5825	12378
	30	75.83	2463	15740
	40	14.86	512	17691
	50	0	0	18203
	60	0	0	18203
	70	0	0	18203
	80	0	0	18203
	90	0	0	18202
H_{det} = 15, p=20, a=120, H=80, C_S=3	0	610.32	18203	0
	10	546.55	17695	508
	20	168.56	5969	12234
	30	89.78	3100	15103
	40	24.71	961	17242
	50	0	0	18203
	60	0	0	18203
	70	0	0	18203
	80	0	0	18203
	90	0	0	18202
H_{det} = 20, p=20, a=120, H=80, C_S=3	0	666.92	18203	0
	10	529	15899	2304
	20	183.15	6944	11259
	30	90.57	3235	14968
	40	35.3	1549	16654
	50	0	0	18203
	60	0	0	18203
	70	0	0	18203
	80	0	0	18203
	90	0	0	18202
H_{det} = 25, p=20, a=120, H=80, C_S=3	0	723.43	18203	0
	10	512.45	14459	3744
	20	205.36	7811	10392
	30	83.92	3140	15063
	40	44.42	2009	16194
	50	2.75	166	18037
	60	0	0	18203
	70	0	0	18203
	80	0	0	18203
	90	0	0	18202

4. INTERPRETATION OF RESULTS

Data in the above tables were plot for a more intuitive interpretation. Figure 6 shows a family of surfaces corresponding to the course of captured energy in respect with the incidence angle θ, by the concentrator with apertures a=60, 70, 80, 90, 100, 110 and 120 mm, for cell positions H_{det} = 10, 15, 20 and 25 mm.

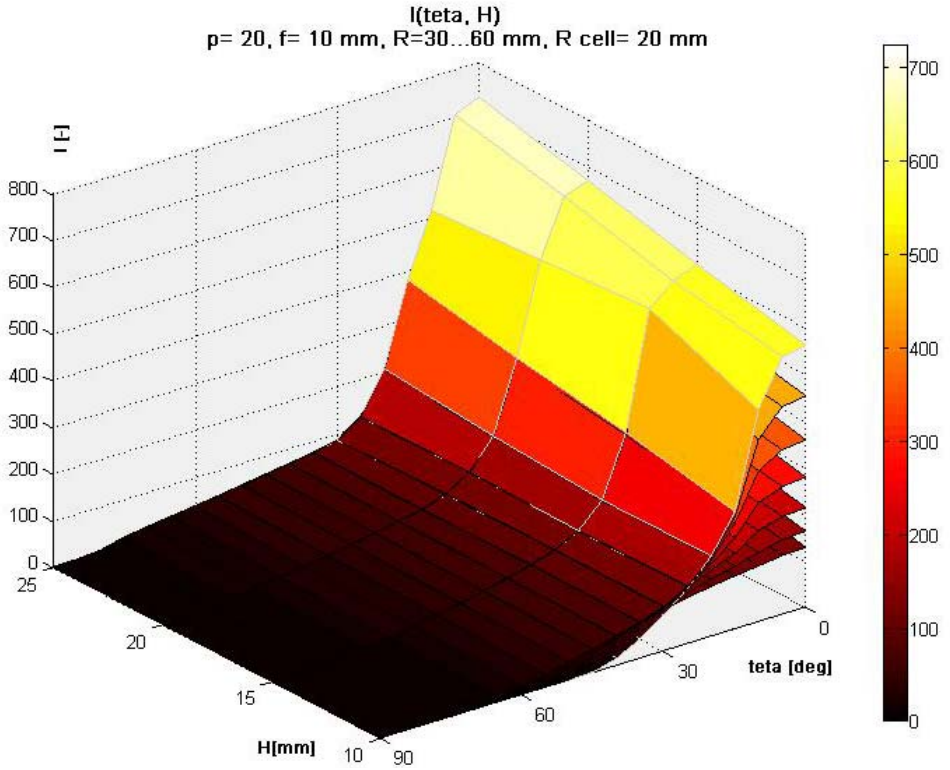

Fig. 6. Course of energy captured in relationship with the angle θ, at apertures a=60, 70, 80, 90, 100, 110 and 120 mm, for H_{det}=10… 25 mm

One can notice an increase of the concentration coefficient C_S proportionally with the aperture and defocusing of the detector to longer abscissa than the paraxial one. Simulations for defocusing bigger than 25 mm indicated a decrease of the optical concentration coefficient. This abscissa (H_{det} = 25 mm) is considered to be optimal for the family of paraboloidal concentrators of constant p=20.

Tables 3…5 allow the study on the course of energy considering a fixed abscissa of the cell and a variable aperture. The family of resulting family of surfaces is represented in figure 7.

The conclusions are similar to the previous ones. The optimal position of the cell corresponds to the abscissa H_{det} =25mm.

Choice of the paraboloidal surface in the family with the constant p=20 is conditioned by optimization criteria regarding global size. One can notice that as the aperture increases the height of the paraboloid grows. From standpoint of surface energy distribution, the best parabolas are wide –opened ones. If there are restrictions regarding the maximum admitted size then the aperture is limited by H.

For all studied variants, the reasonable angle of the active incident beam is approximately 30^o.

In this case the maximum theoretical optical concentration coefficient (for a 3D concentrator) is:

$$C = \frac{2n^2}{\sin^2\theta} = \frac{2}{\sin^2 30^o} = 8, \tag{9}$$

if the system works in the air and the refractive index is n=1.

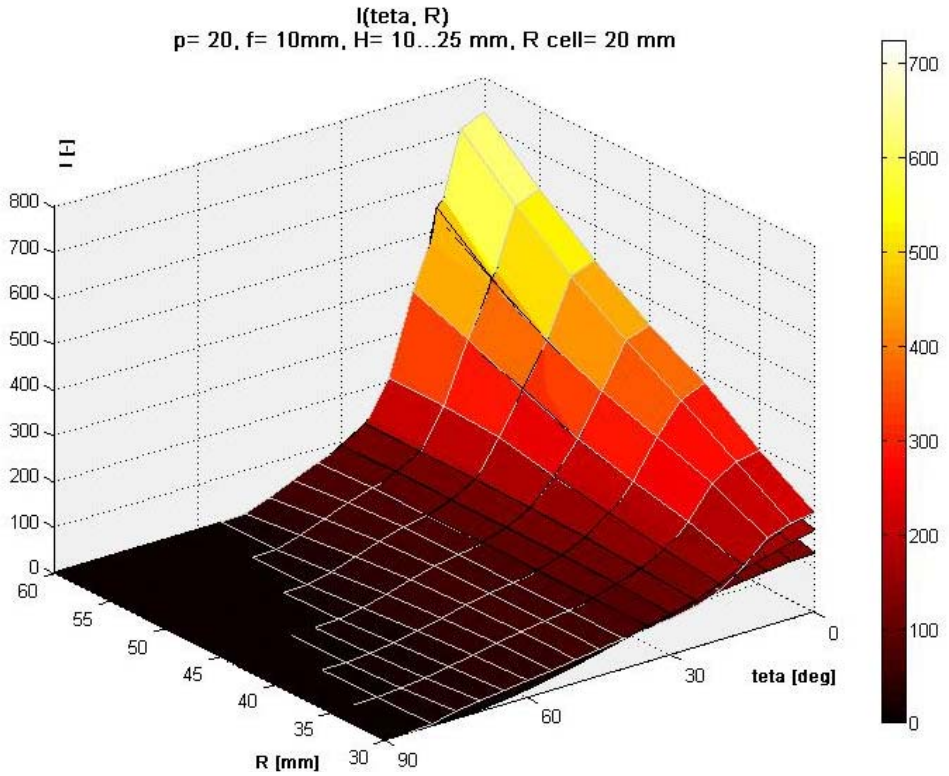

Fig. 7. Course of energy captured in relation with the angle θ, for H_{det}=10, 15, 20, 25 mm, at apertures a=60...120 mm

For the studied example, the optical concentration coefficient is higher than 7 for normal incidence in case a=120 mm and H_{det}=25 mm.

Table 6 and figure 8 emphasise the variation of the optical concentration coefficient at normal incidence, in respect with the aperture, at the optimum position of the cell.

Table 6. Optical concentration coefficient at normal incidence in respect with the aperture at H_{det} = 25 mm

a [mm]	C
60	2.15
70	2.90
80	3.76
90	4.41
100	5.21
110	6.15
120	7.23

5. CONCLUSIONS

The study reveals the importance of geometrical effective characteristics of a paraboloidal 3D solar concentrator. These characteristics are interdependent and demand complex numerical simulations, in which aperture and height are considered, one by one, as parameters.

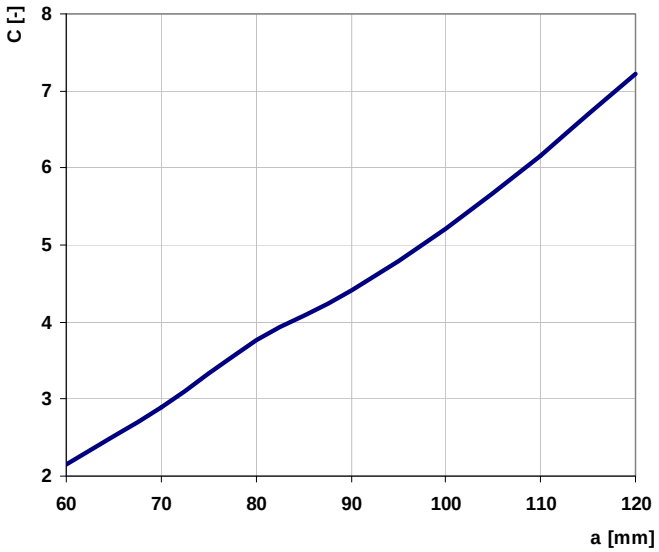

Fig. 8. Variation of the maximum optical concentration coefficient in respect with the aperture

The family of paraboloidal surfaces characterized by a constant *p*, allow the establishment of an optimal position for the receiving cell. The simulations indicated that this position is in the neighbourhood of the paraxial focus. The optimal defocusing is possible to be found by repeated numerical simulations.

A large number of rays, scanning a 90^o field, allow the identification of optimal related sizes aperture – height, at a given position of the cell. The optimization criterion was the optical concentration coefficient.

The paper provided a numerical solution for the geometry of a paraboloidal concentrator assuring an optical concentration coefficient of 8.

REFERENCES

[1] http://en.wikipedia.org/wiki/Photovoltaics
[2] Winston, R., Minano, J.C., Benitez, P., (2005), *Nonimaging optics*, Elsevier Academic Press
[3] Scott, E., (2005), Solar Concentrators, *http://www.parc.com/research/publications/files/5706.pdf*
[4] Coşniță, C., (1965), *Geometria analitică şi diferențială*, în Manualul inginerului, vol. I, Editura Tehnică, Bucureşti
[5] Glassner, A., (1991), *An Introduction to Ray Tracing*, 3rd ed., Academic Press Limited London